

Static configurations and evolution of higher dimensional brane-dilaton black hole system

Anna Nakonieczna,^a Łukasz Nakonieczny,^b Rafał Moderski,^c Marek Rogatko^a

^a*Institute of Physics, Maria Curie-Skłodowska University,
Plac Marii Curie-Skłodowskiej 1, 20-031 Lublin, Poland*

^b*Institute of Theoretical Physics, Faculty of Physics, University of Warsaw,
ul. Pasteura 5, 02-093 Warsaw, Poland*

^c*Nicolaus Copernicus Astronomical Center, Polish Academy of Sciences,
Bartycka 18, 00-716 Warsaw, Poland*

E-mail: aborkow@kft.umcs.lublin.pl, Lukasz.Nakonieczny@fuw.edu.pl,
rogat@kft.umcs.lublin.pl, moderski@camk.edu.pl

ABSTRACT: Static configurations and a dynamical evolution of the system composed of a higher-dimensional spherically symmetric dilaton black hole and the Dirac-Goto-Nambu brane were investigated. The studies were conducted for three values of the dilaton coupling constant, describing the uncoupled case, the low-energy limit of the string theory and dimensionally reduced Klein-Kaluza theories. When the black hole is nonextremal, two types of static configurations are observed, a brane which intersects the black hole horizon and a brane not having any common points with the accompanying black hole. As the number of spacetime dimensions increases, the brane bend in the vicinity of the black hole disappears closer to its horizon. Dynamical evolution of the system results in an expulsion of the black hole from the brane. It proceeds faster for bigger values of the bulk spacetime dimension and thicker branes. The value of the dilatonic coupling constant does not influence neither the static configurations nor the dynamical behavior of the examined nonextremal system. In the extremal dilaton black hole case one obtains expulsion of the brane which is independent on the spacetime dimensionality and the value of the coupling constant. Dynamical studies of the configurations in the extremal case reveal that the course of evolution of the system is similar to the nonextremal one, except for a slightly earlier expulsion of the black hole from the brane.

Contents

1	Introduction	1
2	Bulk spacetime containing a higher-dimensional dilaton black hole	3
3	Static brane-dilaton black hole system	3
3.1	Theoretical setup	3
3.2	Brane behavior in the limiting regions	5
3.3	Spatial configurations	7
4	Evolution of the brane-dilaton black hole system	9
4.1	Theoretical model	10
4.2	Numerical computations	11
4.3	Dynamical behavior	12
5	Conclusions	15

1 Introduction

A resurgence of studies of higher-dimensional black holes, black branes and their mutual interactions has been observed recently. These subjects are valid in several different areas of modern theoretical physics. Contemporary candidates of quantum gravity such as the string/M-theory predict that our universe can be described as a brane embedded in a higher-dimensional spacetime. This idea was incorporated in the so-called brane-world models which are composed of a higher-dimensional bulk and a lower-dimensional embedded brane. The first brane-world models were built with a tensionless brane and compactified flat extra dimensions [1, 2]. Later on, they were extended to the case of a non-zero tension brane and a warped (negatively curved) spacetime [3, 4]. The Standard Model particles are confined to the brane, while gravity can penetrate the other additional dimensions. In such theories interactions between the brane and black holes were intensively investigated [5]. Especially, much attention was paid to the problem of higher-dimensional black holes/black objects crossing the brane and the expulsion problem for such systems. In [6] a toy model for studying a process of merging within the brane-black hole system and a topology change was considered. The higher-dimensional generalizations both in classical general relativity and in certain strongly coupled gauge theories were presented in [7–10].

One of the predictions of the theories with large extra dimensions is the conjecture that mini black holes with masses of 1 TeV can be in principle observed in LHC [11, 12]. Namely, when two particles on the brane collide at the center of mass energy larger than 1 TeV, the system collapses and the formation of mini black hole begins. With the passage of time the

black hole starts to emit Hawking radiation into lower dimensional fields localized on the brane and partly into the higher-dimensional mode, i.e., into the bulk.

The early stages of the evolution of our Universe are also the arenas where primordial black holes and domain walls could have been born. Cosmological density perturbations may have collapsed and led to the formation of small black holes. Next, when the Universe underwent several cooling processes series of phase transitions might occurred leading to the domain wall and other cosmological defects formation [13]. In principle, the interaction of black holes with branes (domain walls) should be taken into account when discussing the aforementioned period of the Universe evolution.

In the past few decades, the interactions between black holes and domain walls have been an object of serious studies, both analytical and numerical. A Nambu-Goto membrane in the Reissner-Nordström-de Sitter spacetime was studied in [14], while the gravitational system of the Schwarzschild static black hole and a thick domain wall was examined in [15, 16]. The domain walls were simulated by a scalar field with an adequate potential like ϕ^4 or the sine-Gordon ones. The dilaton black hole-domain wall system was elaborated in [17, 18]. Among all, it was shown that in the extremal case the expulsion of the scalar field connected with a domain wall took place. In [19] it was revealed that there was a parameter depending on the black hole mass and the width of a domain wall, which turned out to be an upper limit for the expulsion process. The thick domain wall problem in the anti-de Sitter spacetime was treated in [20], while the cosmological brane-black hole system in [21]. By using the C-metric construction the line element describing an infinitely thin brane intersected by a cosmological black hole was derived.

In [22] the black hole whose size was small when compared to the extra dimensions was considered (the tension of the brane was negligible). The simulation was conducted by looking for the dynamical evolution of the brane in the fixed background of the black hole. Further studies of the interaction of a black hole with a scalar field domain wall confirm the previously drawn conclusions [23]. The evolution of the system was also analyzed during the separation process. In [24] the problem of the influence of the brane tension on the escaping black hole was elaborated. The new challenge was to find if the brane tension might prevent the black hole from escaping for a small recoil velocity. The numerical studies of the interaction of black holes with the field theoretical domain wall, i.e., described by an axion-like field theory with an approximate $U(1)$ -gauge symmetry, exploring the topology changing process of a brane perforation was conducted in [25]. It was revealed that the perforation process depends on the collision velocity and there was a critical value of velocity which suppressed the domain wall perforation.

In [26, 27] the studies of the domain walls perforation by black holes envisaged that the mechanism is more or less relevant to the cosmological domain wall case. On the other hand, the curvature corrections to the static axisymmetric membrane evolution in the spherically symmetric spacetime of an arbitrary dimensional black hole, were given in [28]. The problem of a thick brane-black hole system was explored in a series of papers, where perturbative and non-perturbative solutions including the case of a two-brane were studied [28–30]. The last moments of a mini black hole escaping from a brane were examined in [31]. Among all, it was shown that the world sheet becomes isotropic at the reconnection point. It turns

out that the higher dimension we examine, the faster the brane becomes isotropic.

A collision of a point particle with an infinitely thin planar domain wall interacting gravitationally within the linearized gravity in the Minkowski spacetime of an arbitrary dimension was analyzed in [32]. The energy momentum balance in the aforementioned system was found in [33].

In our paper, both static configurations and a dynamical evolution of a brane-dilaton black hole (BDBH) system were investigated. The dilaton black hole was briefly described in section 2 to establish the notations for the bulk spacetime. The studied brane embedded in the black hole spacetime was codimension-one. The theoretical frameworks of the above-mentioned static and dynamical setups, along with computational details and results were presented in sections 3 and 4, respectively. The summary of our findings was presented in section 5.

2 Bulk spacetime containing a higher-dimensional dilaton black hole

The considered black hole was a d -dimensional dilaton black hole, whose metric in (t, r, θ_i) coordinates, where $i = 1, \dots, d - 2$, is given by [34]

$$ds^2 = - \left[1 - \left(\frac{r_+}{r} \right)^{d-3} \right] \left[1 - \left(\frac{r_-}{r} \right)^{d-3} \right]^{1-\gamma(d-3)} dt^2 + \\ + \left[1 - \left(\frac{r_+}{r} \right)^{d-3} \right]^{-1} \left[1 - \left(\frac{r_-}{r} \right)^{d-3} \right]^{\gamma-1} dr^2 + r^2 \left[1 - \left(\frac{r_-}{r} \right)^{d-3} \right]^\gamma d\Omega_{d-2}^2, \quad (2.1)$$

where r_+ and r_- are the radii of two horizons, the outer and inner ones, $r_+ > r_-$. The case when $r_+ = r_-$ is reserved for the extremal higher-dimensional dilaton black hole. Ω_{d-2}^2 is the line element of the $d - 2$ -dimensional unit sphere with coordinates θ_i , $i = 1, \dots, d - 2$, defined on it by the relations $d\Omega_{i+1}^2 = d\theta_{i+1}^2 + \sin^2 \theta_{i+1} d\Omega_i^2$. γ is an auxiliary constant related to the dilaton coupling constant α and the dimension of the considered spacetime d by the following relation:

$$\gamma = \frac{2\alpha^2(d-2)}{(d-3)[2(d-3) + \alpha^2(d-2)]}. \quad (2.2)$$

For the brevity, two functions $f_1 = 1 - \left(\frac{r_+}{r} \right)^{d-3}$ and $f_2 = 1 - \left(\frac{r_-}{r} \right)^{d-3}$ will be used throughout the paper.

3 Static brane-dilaton black hole system

3.1 Theoretical setup

In this section we shall pay attention to a static brane - higher dimensional static spherically symmetric black hole system. A brane $(D - 1)$ -dimensional configuration in a gravitational field of a black object will be analyzed having in mind the Dirac-Nambu-Goto action [35–37]

$$S = \int d^D \zeta \sqrt{-\det \gamma_{ij}}, \quad (3.1)$$

where ζ^i , $i = 0, \dots, D-1$, are the coordinates on the brane world sheet and the D -dimensional metric induced on the world sheet is given by

$$\gamma_{ij} = g_{\mu\nu} X_{,i}^{\mu} X_{,j}^{\nu} \quad (3.2)$$

with X^{μ} , $\mu = 0, \dots, d-1$, being the bulk spacetime coordinates. In the case of a codimension-one brane $D = d$.

The assumption that the brane is static and spherically symmetric results in an $O(D-1)$ symmetry of its world sheet. The world sheet is thus defined by the function $\theta_{D-1} \equiv \theta(r)$, with $\theta_i = \frac{\pi}{2}$ for $i = D, \dots, d-2$. The metric induced on the brane world sheet has the form

$$ds^2 = -f_1 f_2^{1-\gamma(n-3)} dt^2 + \left[\frac{f_2^{\gamma-1}}{f_1} + r^2 f_2^{\gamma} \left(\frac{d\theta}{dr} \right)^2 \right] dr^2 + r^2 f_2^{\gamma} \sin^2 \theta d\Omega_n^2, \quad (3.3)$$

where $n = D-2$. The action (3.1) reduces to

$$S = \Delta T \mathcal{A} \int dr \mathcal{L} \quad (3.4)$$

with the Lagrange density provided by

$$\mathcal{L} = r^n \sin^n \theta f_2^{\frac{\gamma n}{2}} \left[f_2^{\gamma(4-n)} + r^2 f_1 f_2^{1-\gamma(n-4)} \left(\frac{d\theta}{dr} \right)^2 \right]^{\frac{1}{2}}, \quad (3.5)$$

where ΔT is the time interval and \mathcal{A} is the surface of a unit n -dimensional sphere.

Static configurations of the brane-dilaton black hole system are determined by the Lagrange equation

$$\frac{d}{dr} \left(\frac{\partial \mathcal{L}}{\partial \theta'} \right) - \frac{\partial \mathcal{L}}{\partial \theta} = 0, \quad (3.6)$$

where $'$ denotes the differentiation with respect to the r -coordinate. An explicit form of the equation is provided by

$$\frac{d^2 \theta}{dr^2} + A_1 \left(\frac{d\theta}{dr} \right)^3 + A_2 \left(\frac{d\theta}{dr} \right)^2 + A_3 \left(\frac{d\theta}{dr} \right) + A_4 = 0, \quad (3.7)$$

where by A_i , $i = 1, \dots, 4$, we have denoted the following:

$$\begin{aligned} A_1 &= r(n+1)f_1 f_2 + \frac{r^2}{f_2^{\gamma(4-n)+\frac{\gamma n}{2}}} \frac{d}{dr} \left(f_1 f_2^{1-\gamma(n-4)+\frac{\gamma n}{2}} \right) + \\ &\quad - \frac{1}{2} \frac{r^2}{f_2^{\gamma(4-n)}} \frac{d}{dr} \left(f_1 f_2^{1-\gamma(n-4)} \right) = \\ &= r(n+1)f_1 f_2 + \frac{r^2}{2} f_2 \frac{df_1}{dr} + \frac{r^2}{2} (1+4\gamma) f_1 \frac{df_2}{dr}, \end{aligned} \quad (3.8)$$

$$A_2 = -n \cot \theta, \quad (3.9)$$

$$\begin{aligned} A_3 &= \frac{n+2}{r} + \frac{1}{f_1 f_2^{1-\frac{\gamma n}{2}+4\gamma}} \frac{d}{dr} \left(f_1 f_2^{1-\frac{\gamma n}{2}+4\gamma} \right) - \frac{1}{2 f_2^{\gamma(4-n)}} \frac{d}{dr} \left(f_2^{\gamma(4-n)} \right) = \\ &= \frac{n+2}{r} + \frac{1}{f_1} \frac{df_1}{dr} + (1+2\gamma) \frac{1}{f_2} \frac{df_2}{dr}, \end{aligned} \quad (3.10)$$

$$A_4 = -\frac{n \cot \theta}{r^2 f_1 f_2}. \quad (3.11)$$

The equation (3.7) possesses singular points at the black hole horizon and at infinity. In order to derive static configurations of the considered system, the behavior of the brane in the two limiting regions, i.e., $r \rightarrow r_+$ and $r \rightarrow \infty$, has to be determined. This behavior gives appropriate boundary conditions for the θ function, which differ for nonextremal and extremal black holes. The boundary behavior will be discussed for the nonextremal BDBH system and then the differences relevant to the extremal case will be pointed out.

3.2 Brane behavior in the limiting regions

In principle, there exist two possible configurations of the brane in the near horizon limit $r \rightarrow r_+$, which are the brane penetrating and not touching the black hole event horizon. The analysis of the penetrating solution reveals the singular coefficients in the equation (3.7) which are composed of the part of the second expression in (3.10) and the A_4 coefficient. Hence, the singular part of the considered equation is of the form

$$\tilde{A}_3 \theta' + A_4, \quad (3.12)$$

where $\tilde{A}_3 = f_1^{-1} f_1'$. It can be written as

$$\frac{f_1' \theta' - n \frac{\cot \theta}{r^2 f_2}}{f_1} \sim \frac{0}{0}, \quad (3.13)$$

where the right-hand side of the above relation is connected with the regularity demand. The above expression yields

$$\left(f_1' \theta' - n \frac{\cot \theta}{r^2 f_2} \right) \Big|_{r=r_+} = 0. \quad (3.14)$$

Postulating that $\theta|_{r \rightarrow r_+} \approx \theta_0 + \theta_1(r - r_+)$, we get that θ_0 is an arbitrary constant and

$$\theta_1 = \frac{n \cot \theta_0}{f_1' r^2 f_2} \Big|_{r=r_+}. \quad (3.15)$$

The above analysis gives both the form of the boundary condition on the horizon $\theta = \text{const.}$ and the near horizon behavior of θ which is helpful in a numerical integration of the discussed equation.

In the case when the brane does not touch the black hole horizon, the input parameter dictating the boundary condition is the minimal distance between the brane and the origin of the coordinate system, r_0 . Due to the symmetry of the system, this distance should be attained for $\theta = 0$, which again leads to the singularity of the equation (3.7) in the $\cot \theta$ term. Postulating that $\theta|_{r \rightarrow r_0} \approx \eta_0(r - r_0)^{\frac{1}{2}} + \eta_1(r - r_0)^{\frac{3}{2}}$, plugging it into the relation (3.7) and expanding the θ -dependent term around $r = r_0$, the following relations for the η_0 and η_1 coefficients arise:

$$\eta_0 = \pm \sqrt{\frac{2}{A_1}(1 - a_2)} \Big|_{r=r_0}, \quad (3.16)$$

$$\eta_1 = \pm \frac{2\sqrt{2}(1 - a_2) \left[a_2 - 2a_2^2 + a_2^3 + 3A_1 a_2 A_3 - 3A_1 (A_3 + A_1 a_4) \right]}{9A_1^{\frac{3}{2}} (3 - 4a_2 + a_2^2)} \Big|_{r=r_0}, \quad (3.17)$$

where a_2 and a_4 are the θ -independent parts of A_2 and A_4 , respectively.

Having specified the behavior of the investigated function in the near horizon limit, we will turn to the $r \rightarrow \infty$ one. Assuming that the brane behaves in this limit as a $d - 1$ -dimensional plane we may write

$$\theta = \frac{\pi}{2} + \lambda(r). \quad (3.18)$$

Moreover, it is assumed that the solution approaches $\theta = \frac{\pi}{2}$ at least as fast as $\frac{1}{r}$. An analysis of the coefficients of the considered equation (3.8)–(3.11) leads to the relations

$$A_1 \sim r^2, \quad (3.19)$$

$$A_2 \sim n\lambda(r), \quad (3.20)$$

$$A_3 \sim \frac{n+2}{r} - (n-1)r_+^{n-1}r^{-n} - (n-1)(1+2\gamma)r_-^{n-1}r^{-n}, \quad (3.21)$$

$$A_4 \sim \frac{n}{r^2}\lambda(r). \quad (3.22)$$

Since λ decays like $\frac{1}{r}$ or faster by definition, the equation (3.7) becomes

$$\lambda'' + \left[\frac{n+2}{r} - (n-1)r_+^{n-1}r^{-n} - (n-1)(1+2\gamma)r_-^{n-1}r^{-n} \right] \lambda' + \frac{n}{r^2}\lambda = 0. \quad (3.23)$$

The second and third terms in the square bracket are relevant only for $d = 3$, as for the bigger number of dimensions they decay as r^{-2} or faster and thus are irrelevant. This implies that for $d \geq 4$ a charged brane behaves in the limit of $r \rightarrow \infty$ like an uncharged one. In this case the solution to the equation (3.23) is given by

$$\lambda = c_1 r^{-1} + c_2 r^{-n}, \quad (3.24)$$

where c_1 and c_2 are integration constants. In the case of $d = 3$ we have $n = 1$ and despite the fact that the terms r^{-n} are relevant, the coefficients in front of them vanish. So the solution is again the same as in the uncharged case and is provided by [6]

$$\lambda = c_1 r^{-1} + c_2 \frac{\ln r}{r}. \quad (3.25)$$

When an extremal dilaton black hole is present in the BDBH system, the behavior of the brane at infinity and near the horizon when the two coexisting objects are separated is the same as discussed above for the nonextremal case. On the other hand, for the brane touching the degenerate horizon the regularity condition implies

$$\frac{\left[f_2 f_1' + (1+2\gamma) f_1 f_2' \right] \theta' - \frac{n \cot \theta}{r^2}}{f_1 f_2} \sim \frac{0}{0}. \quad (3.26)$$

It was derived analogously to the nonextremal case and it implies that $\cot \theta = 0$. Together with an assumption $\theta(r) \approx \theta_0 + \theta_1(r - r_+)$ it gives that $\theta_0 = \frac{\pi}{2}$. Using the L'Hospital rule

once results in the relation

$$\begin{aligned} & \frac{\left[f_2 f_1' + (1 + 2\gamma) f_1 f_2' \right] \theta''}{f_1' f_2 + f_1 f_2'} + \quad (3.27) \\ & + \frac{\left[f_2' f_1' + f_2 f_1'' + (1 + 2\gamma) f_1' f_2' + (1 + 2\gamma) f_1 f_2'' \right] \theta' + \frac{2n \cot \theta}{r^3} + \frac{n}{r^2 \sin^2 \theta} \theta'}{f_1' f_2 + f_1 f_2'} \sim \frac{0}{0}. \end{aligned}$$

Since $f_1(r_+) = f_2(r_+) = 0$, the coefficient in the front of the second derivative of θ , trivially vanishes. Vanishing of the nominator of the second component yields

$$\theta_1 = -\frac{2n \cot \theta_0}{r_+^2} \left[\frac{n}{r_+^2 \sin^2 \theta_0} + 2(1 + \gamma) f_1' f_2' \right]^{-1}, \quad (3.28)$$

where the expansion $\theta|_{r \rightarrow r_+} \approx \theta_0 + \theta_1(r - r_+)$ was employed. The trigonometric functions of θ were also expanded and only the leading terms were kept. Since θ_0 is already fixed to be equal to $\frac{\pi}{2}$, we conclude that $\theta_1 = 0$. Hence, in the extremal case the brane will either not touch the black hole horizon or will touch it precisely at one point on the equator. Moreover, in the last case the brane configuration is given by $\theta = \frac{\pi}{2}$. Due to the near horizon behavior of the brane this is true for any spacetime dimension d and an arbitrary dilatonic coupling constant α .

3.3 Spatial configurations

The static spatial arrangements of the BDBH system were investigated for the bulk spacetime dimensions 5, 6, 7 and 8 and the dilatonic coupling constant equal to 0, -1 and $-\sqrt{3}$. The studied values of α -coupling constant referred to the uncoupled dilaton field, the low energy limit of the string theory and the dimensionally reduced Kaluza-Klein theory, respectively. Each brane configuration in the black hole spacetime will be depicted as a function $\theta(r)$ via cylindrical coordinates $Z = r \cos \theta$, $R = r \sin \theta$.

The configurations of the static nonextremal brane-dilaton black hole system are presented in figures 1 and 2. The nonextremal black hole admits a brane which intersects its horizon and hence both near horizon configurations mentioned in the previous section are observed in this case. The non-penetrating configurations correspond to various values of the parameter r_0 , and the intersecting branes are related to different values of θ_0 . The value of the dilatonic coupling constant does not impact the static configurations. The number of spacetime dimensions influences the brane location in the black hole spacetime such that the brane bend in the vicinity of the black hole horizon disappears closer to it as d increases. It will be interesting to propose the physical interpretation of the observed property. Because of the fact that gravity can penetrate the additional dimensions, its strength is weaker in the case of the growth of the dimensionality of the underlying spacetime, comparing to the gravity force exerted by black hole in four-dimensions. Therefore the increase of the spacetime dimensions (decrease of the gravity force which should penetrate the additional dimensions) is responsible for the closer to the event horizon disappearance of the brane. The very similar situation was revealed in [38]-[40], where it was found that the absorption probability of massive Dirac fermions in the spacetime of higher-dimensional

Schwarzschild black hole and a tense brane black hole, decreased with the increase of the spacetime dimensionality.

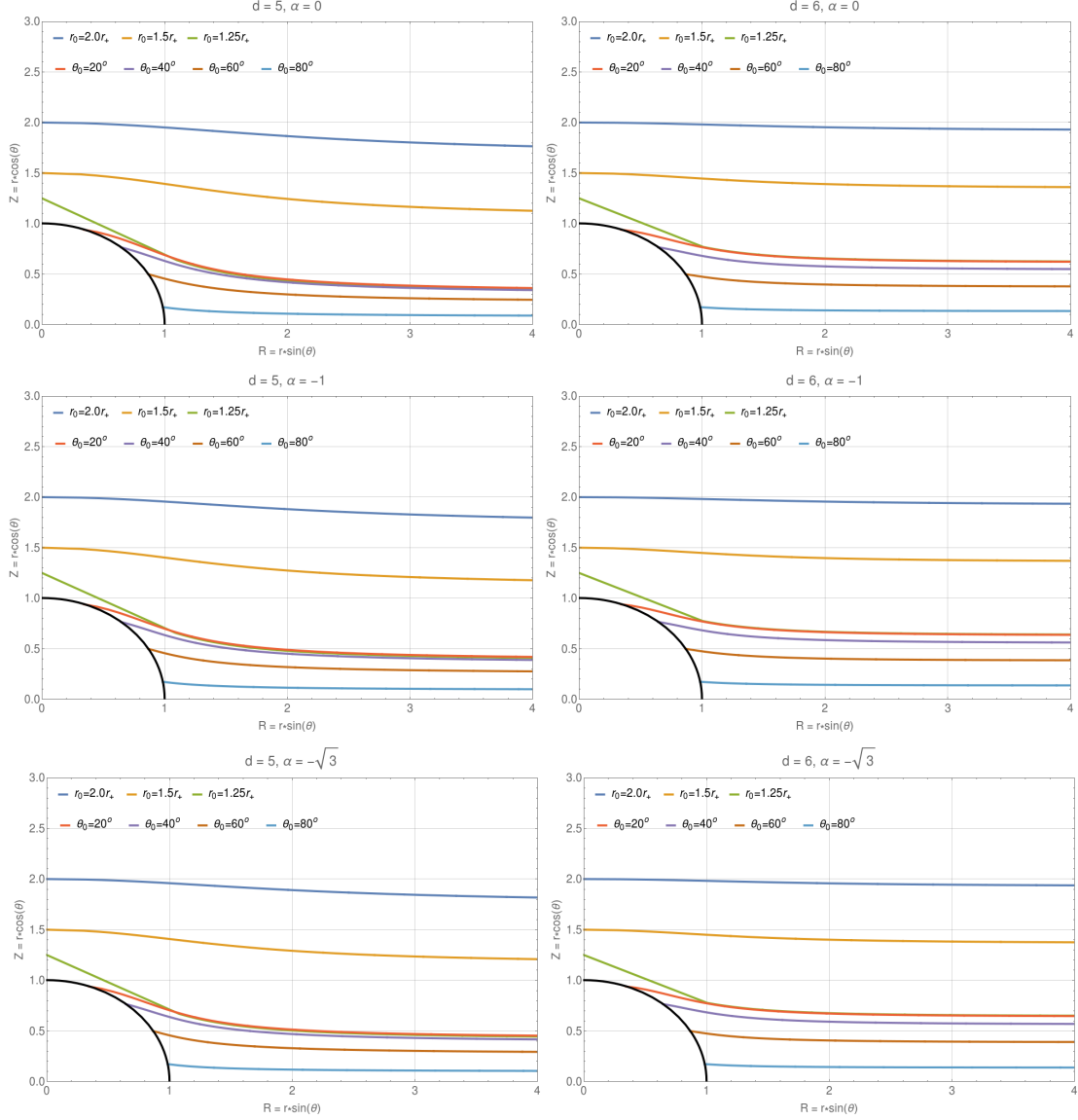


Figure 1. Static configurations of the BDBH system with a nonextremal black hole for d equal to 5 and 6. The spacetime dimension and the value of the coupling constant α are presented above each diagram. The parameters r_0 and θ_0 corresponding to the particular brane locations are listed on the plots.

The static configurations of an extremal brane-dilaton black hole system are depicted in figure 3. Disregarding the values of d and α , there exists only one brane location which penetrates the horizon and it corresponds to the brane situated on the equator plane of the black hole, with $\theta_0 = \frac{\pi}{2}$ and hence $\theta = \frac{\pi}{2}$. The remaining arrangements represent branes which do not have any common points with the horizon. Each of these branes is described by a different value of r_0 . Similarly to the nonextremal case, the bend of

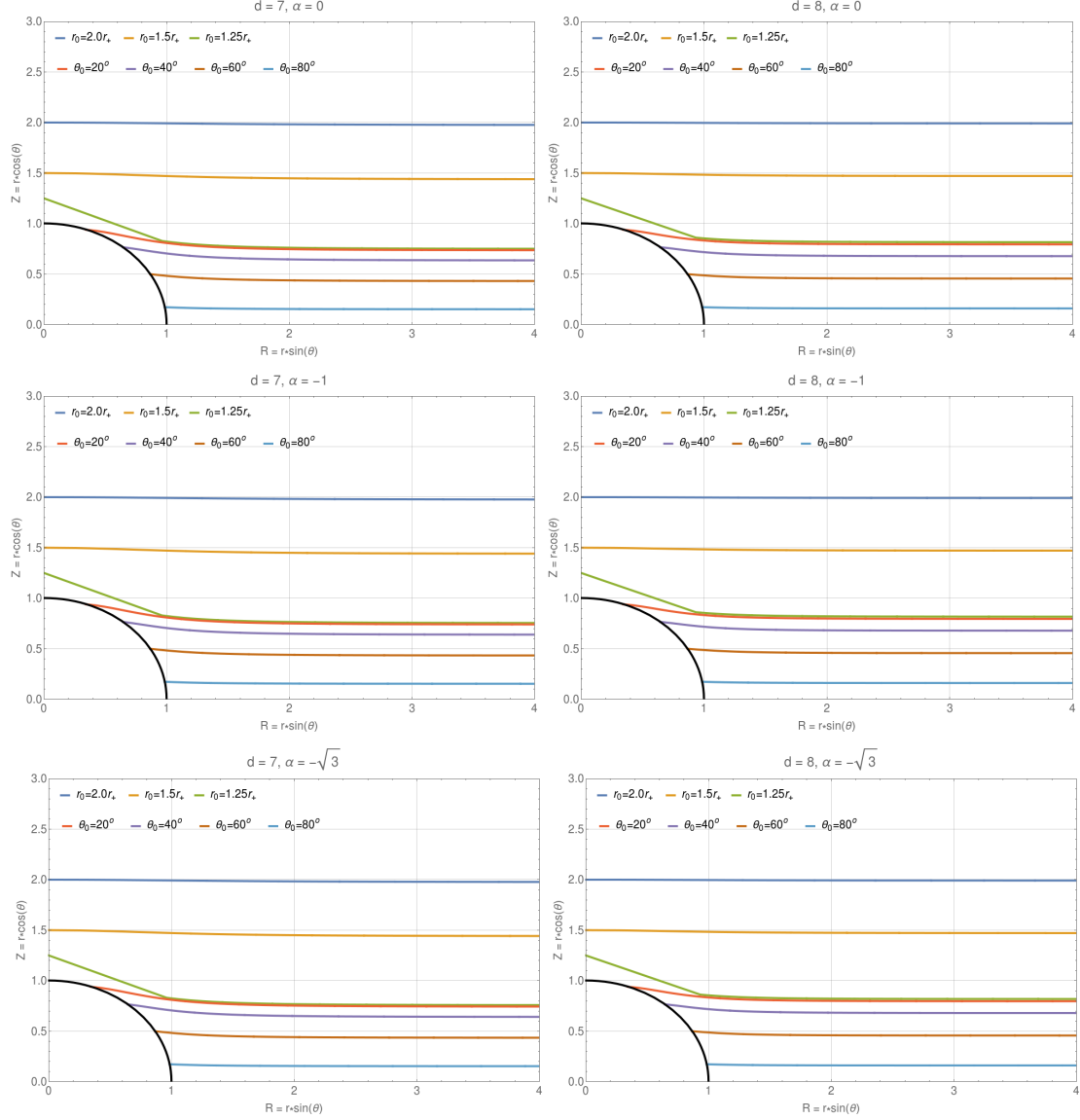


Figure 2. Static configurations of the BDBH system with a nonextremal black hole for d equal to 7 and 8. The spacetime dimension and the value of the coupling constant α are presented above each diagram. The parameters r_0 and θ_0 corresponding to the particular brane locations are listed on the plots.

the brane disconnected with a black hole becomes smaller nearby its event horizon as the dimensionality of the considered spacetime d increases.

4 Evolution of the brane-dilaton black hole system

Our further investigations concentrated on the dynamics of the BDBH system. The tension of the domain wall was assumed to be small which allowed us to ignore its self-gravitation effect.

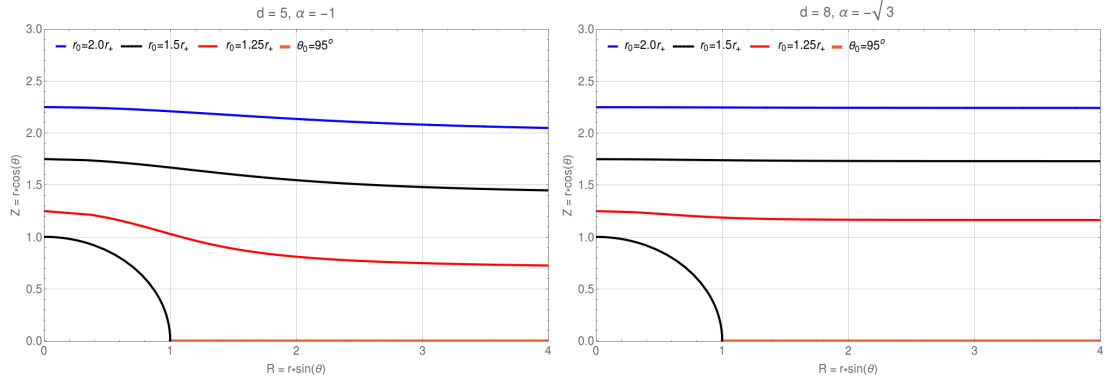


Figure 3. Static configurations of the BDBH system with an extremal black hole. The spacetime dimension d and the value of the coupling constant α are presented above each diagram. The parameters r_0 and θ_0 corresponding to the particular brane locations are listed on the plots.

4.1 Theoretical model

When describing the brane, we confined our attention to a scalar effective field theory with a quadratic potential of the scalar field Φ given by the relation

$$V(\Phi) = \frac{\lambda}{4} (\Phi^2 - \eta^2)^2, \quad (4.1)$$

where the parameters are related to the tension of a domain wall solution in a flat space $\sigma \approx \sqrt{\lambda}\eta^3$ and its thickness $l \approx (\sqrt{\lambda}\eta)^{-1}$.

The equation of motion of the domain wall intersecting the dilaton black hole completely immersed in the higher-dimensional spacetime yields

$$\nabla_\mu \nabla^\mu \Phi - \frac{\partial V}{\partial \Phi} = 0. \quad (4.2)$$

If one assumes an $O(d-2)$ -rotational symmetry around the axis perpendicular to the equatorial plane of the considered black hole, then the following explicit form of the equation of motion arises:

$$\frac{-1}{f_1 f_2^{1-\gamma(d-3)}} \partial_t^2 \Phi + \frac{1}{r^{d-2} f_2^\gamma} \partial_r (r^{d-2} f_1 f_2 \partial_r \Phi) + \frac{1}{r^2 (\sin \theta)^{d-3}} \partial_\theta [(\sin \theta)^{d-3} \partial_\theta \Phi] - \frac{\partial V}{\partial \Phi} = 0. \quad (4.3)$$

Our main aim was to examine the potential recoil of the dilaton black hole from the brane during a dynamical process, at the beginning of which the brane intersecting the black hole acquires an initial velocity. Therefore, Φ and $\partial_t \Phi$ for $t=0$ are given by a static kink profile boosted in the direction of the symmetry axis [23]. Namely, one has

$$\Phi_v = \eta \tanh \left(\sqrt{\frac{\lambda}{2}} \eta \frac{r \cos \theta - vt}{\sqrt{1-v^2}} \right), \quad (4.4)$$

where v is constant.

At infinity, the field describing the brane reduces to the case of a flat spacetime form given by the relation (4.4), while the regularity conditions at the symmetry axis and on the black hole event horizon are

$$\begin{aligned}\frac{\partial\Phi}{\partial\theta} &= 0 \quad \text{at } \theta = 0, \pi, \\ \frac{\partial\Phi}{\partial t} &= 0 \quad \text{at } r = r_+.\end{aligned}\tag{4.5}$$

4.2 Numerical computations

The equation of motion of the scalar field representing the brane (4.3) was solved using the collocation spectral method [41] in the spatial directions r and θ . The temporal evolution was conducted via a finite difference scheme based on three adjacent $t = \text{const.}$ hypersurfaces.

The applied pseudospectral method required writing the equation to be solved using a polynomial expansion of an unknown function at the so-called collocation points. The points were spread on a grid, which spanned from -1 to 1 in the spectral directions, which in the considered case were r and θ .

The general form of Φ was chosen as an expansion in terms of the Chebyshev polynomials of the first kind

$$\Phi(t, y(r), x(\theta)) = \sum_{m=0}^M \sum_{n=0}^N \varphi_{mn}(t) T_m(y) T_n(x),\tag{4.6}$$

where $y = \frac{r-2r_+-1}{r+1}$ and $x = \cos\theta$ are the independent spatial variables rescaled to the range $[-1, 1]$, which is necessary for applying the pseudospectral method. The time dependent expansion coefficients were denoted as φ_{mn} . The applied expansion involved 50 Chebyshev polynomials in each of the two spatial directions. The collocation points were of the Gauss-Lobatto type, i.e, they were spread on the computational grid, in each of the spectral directions, according to a prescription

$$z_k = -\cos\frac{k\pi}{K},\tag{4.7}$$

where $k = 0, \dots, K$, z stands for either y or x and K denotes M or N , respectively.

The equation of motion of Φ (4.3) was reduced by applying the expansion (4.6) to the evolution equation of the expansion coefficients φ_{mn} and obtained the form

$$\begin{aligned}\sum_m \sum_n \ddot{\varphi}_{mn}(t) T_m(y) T_n(x) - \frac{(1-y)^d f_1 f_2^{1-\gamma(d-2)}}{2(r_++1)(2r_++1+y)^{d-2}} \sum_m \sum_n \varphi_{mn}(t) T_n(x) L_m(y) + \\ - \frac{(1-y)^2 f_1 f_2^{1-\gamma(d-3)}}{(2r_++1+y)^2} \sum_m \sum_n \varphi_{mn}(t) T_m(y) L_n(x) + f_1 f_2^{1-\gamma(d-3)} \frac{dV}{d\Phi} = 0,\end{aligned}\tag{4.8}$$

where a dot is a derivative with respect to the t -coordinate and the auxiliary quantities are the following:

$$L_m(y) = \frac{(2r_+ + 1 + y)^{d-3} \left[d - 2 - \frac{(d-4)(2r_+ + 1 + y)}{1-y} \right]}{2(r_+ + 1)(1-y)^{d-4}} f_1 f_2 \partial_y T_m(y) + \frac{(2r_+ + 1 + y)^{d-2}}{2(r_+ + 1)(1-y)^{d-4}} \left[(\partial_y f_1 f_2 + f_1 \partial_y f_2) \partial_y T_m(y) + f_1 f_2 \partial_y^2 T_m(y) \right], \quad (4.9)$$

$$L_n(x) = (2-d)x \partial_x T_n(x) + (1-x^2) \partial_x^2 T_n(x). \quad (4.10)$$

The equation (4.8) was written at each of the collocation points (4.7) separately. The resulting system of algebraic equations for the unknown φ_{mn} was solved on each time step with the use of the LU decomposition method [45].

The pseudospectral method provides an exact solution at the collocation points. Since the overall solution is approximated by a set of polynomials, bumps can appear in the regions between the points. They are an artifact of the numerical scheme. The density of the grid, i.e., the amount of collocation points used in our setup (50 in each spatial direction), ensured a very good accuracy of the obtained outcomes and facilitated their interpretation. It was also sufficient for modeling the step-type profile of the scalar field (4.4), which was necessary for reflecting the existence of the brane in the spacetime.

4.3 Dynamical behavior

The location of the brane in the spacetime was determined taking into account the values of the energy density of the scalar field Φ

$$T_0^0 = \frac{1}{f_1 f_2^{1-\gamma(d-3)}} (\partial_t \Phi)^2 + \frac{1}{4} f_1 f_2^{1-\gamma} (\partial_r \Phi)^2 + \frac{1}{r^2} (\partial_\theta \Phi)^2 + \frac{1}{2} V(\Phi). \quad (4.11)$$

The results of the computations are presented through series of snapshots of the temporal evolution of the brane-black hole system. Each of the plots shows the energy density of the scalar field (4.11) within the black hole spacetime in cylindrical coordinates. The locations of the black hole horizons and the number of the evolution time step are shown on each diagram.

The investigated spacetime dimensions were 4, 5, 6, 7 and 8. The brane thickness l was set as 0.1, 0.3 and 0.4, while its initial velocity v was assumed to be equal to 0.1, 0.3 and 0.7. Similarly to the case of static configurations of the BDBH system described in section 3, three values of the dilatonic constant α were considered, namely $-\sqrt{3}$, -1 and 0 . The constant η was equal to 0.1 in all simulations, which in addition to the value of l determined the tension of the domain wall in each of the investigated cases.

Figures 4–7 present the dependence of the dynamical behavior of the brane-black hole system on d , l , v and α , respectively, in the case of a nonextremal black hole with $r_- = 0.1$ and $r_+ = 0.5$. In all cases, the plane within which the brane was located initially divided the black hole into two hemispheres. Since the brane acquired a non-zero velocity at the beginning of the investigated process, with the passage of time it moved in a specific

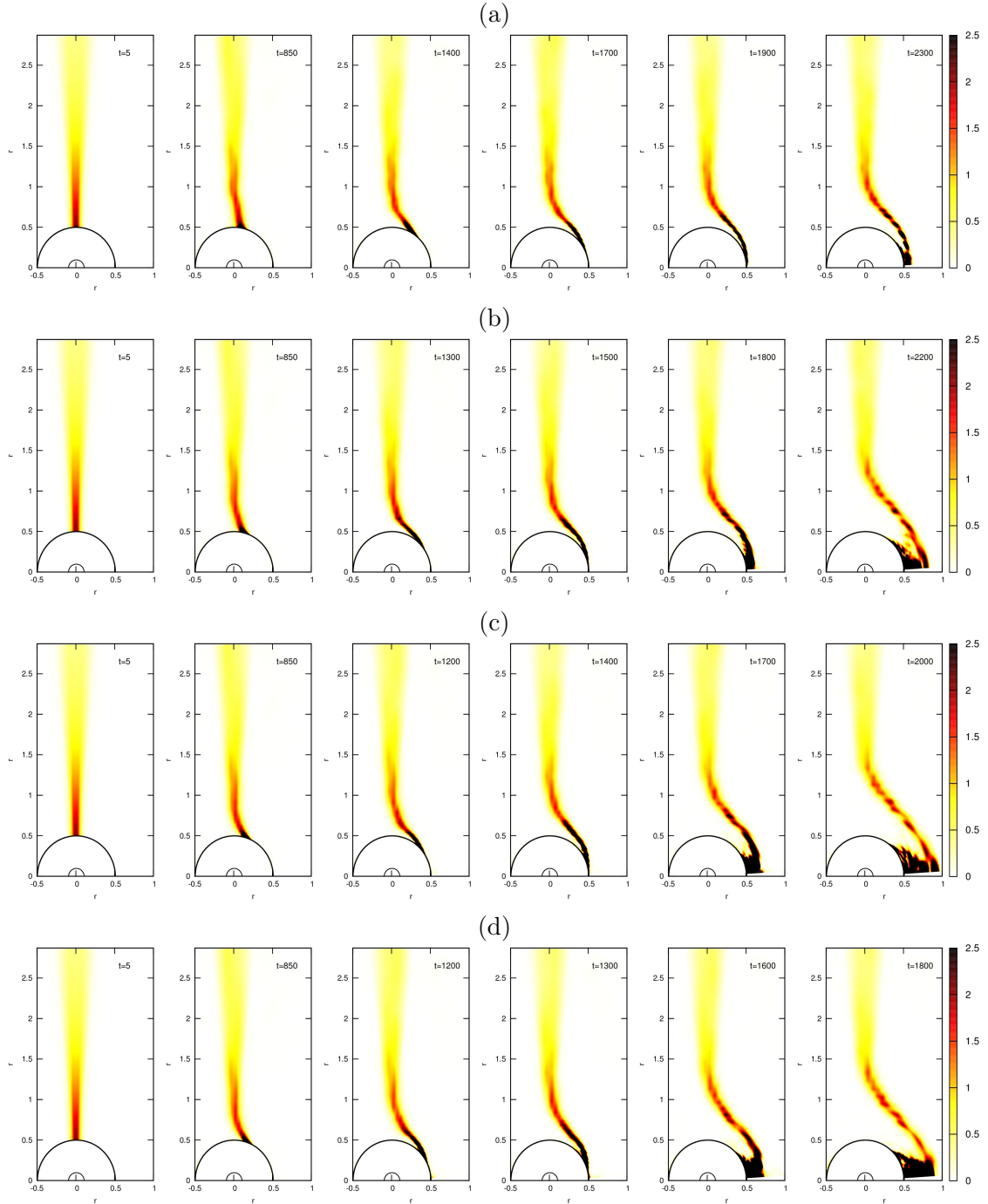


Figure 4. The evolution of the BDBH system with the nonextremal black hole for d equal to (a) 4, (b) 5, (c) 6 and (d) 7. The remaining parameters were set as $l = 0.1$, $v = 0.1$ and $\alpha = -1$.

direction. Such a situation can also be interpreted as a black hole being expelled from the brane.

The research conducted for a BDBH system containing a nonextremal black hole revealed that the expulsion appears earlier for larger d and the black hole is expelled earlier

from a thicker brane (with bigger l). The radius of the area of the brane deformation is bigger for a thicker brane, it moves away from the initial position within a larger distance from the black hole. The energy density associated with a thick brane is smaller in comparison to a thin brane. Bigger initial velocity of the brane results in an earlier expulsion of the black hole and causes an increase of the radius of the area of the brane deformation nearby the black hole. The dynamics of the studied brane-black hole system does not depend on the value of α .

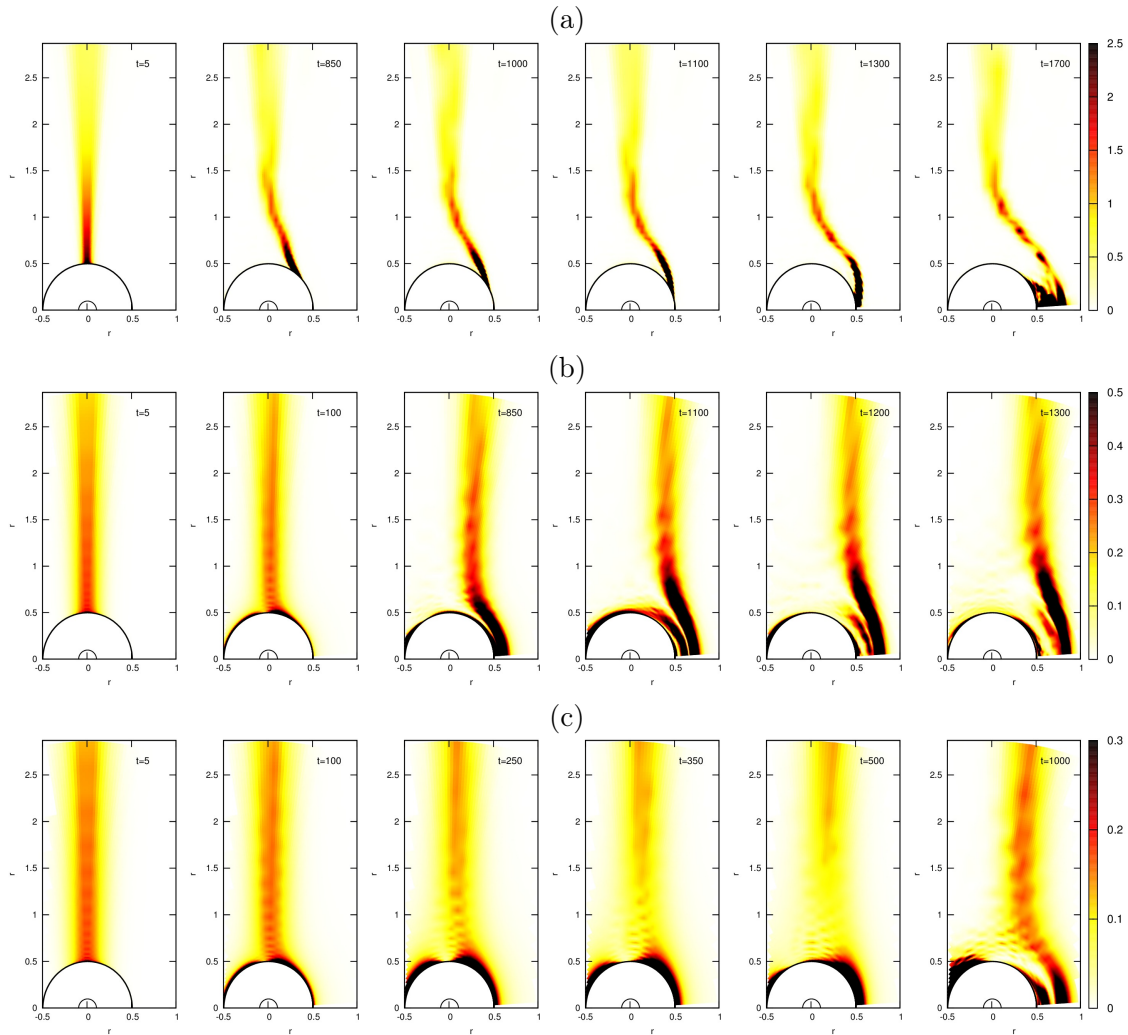


Figure 5. The evolution of the BDBH system with the nonextremal black hole for l equal to (a) 0.1, (b) 0.3 and (c) 0.4. The remaining parameters were set as $d = 5$, $v = 0.3$ and $\alpha = 0$.

The evolution of the examined system was also followed for an extremal black hole with $r_- = r_+ = 0.5$. The outcomes were qualitatively the same as in the nonextremal case, the only difference was that the expulsion appeared a bit earlier in the extremal case.

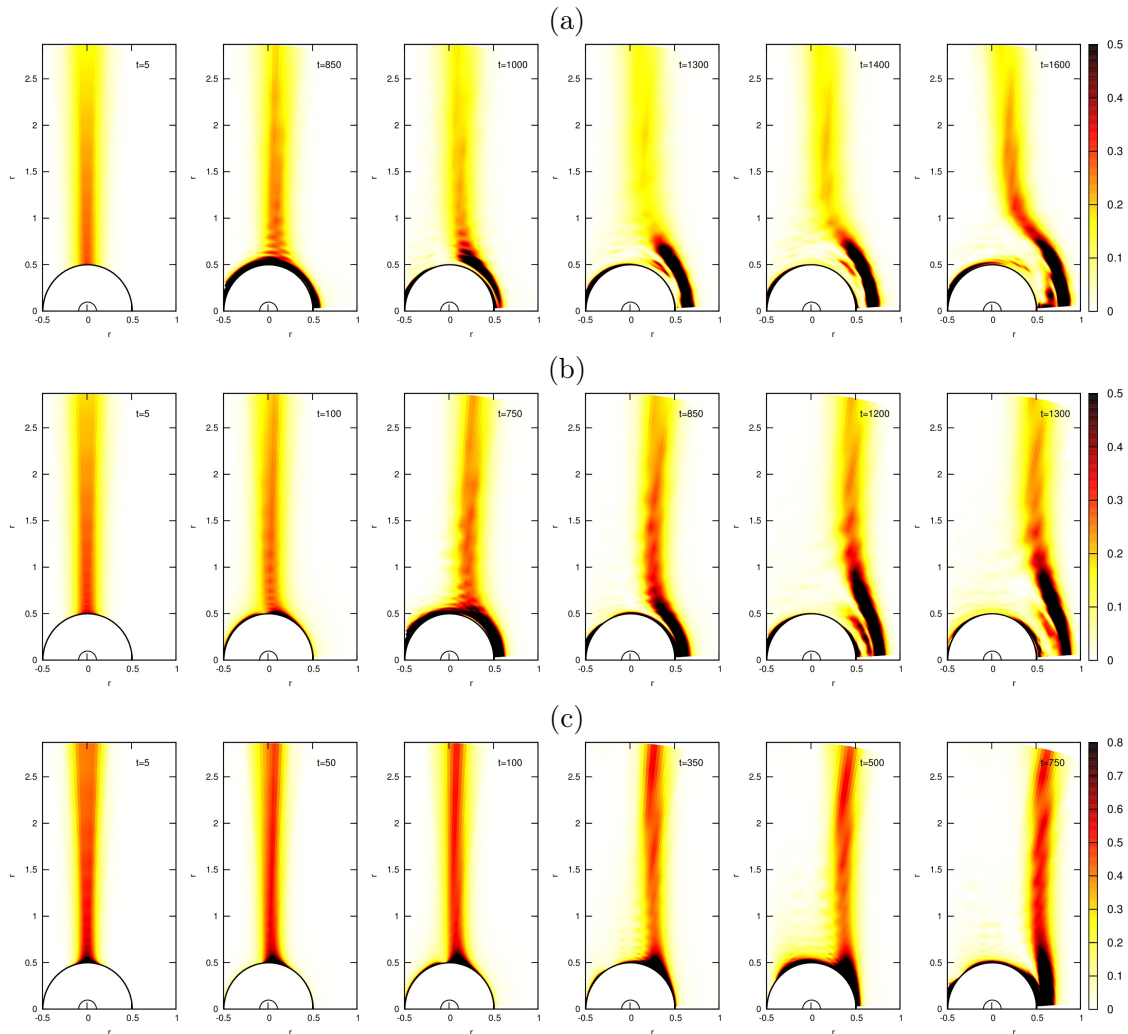


Figure 6. The evolution of the BDBH system with the nonextremal black hole for v equal to (a) 0.1, (b) 0.3 and (c) 0.7. The remaining parameters were set as $d = 5$, $l = 0.3$ and $\alpha = -1$.

5 Conclusions

In our paper we pay attention to static configurations and a dynamical evolution of the system consisting of a higher-dimensional spherically symmetric dilaton black hole and a Goto-Nambu type brane.

The studies were conducted for three values of the coupling constant α , which were referred to the uncoupled dilaton field, the low-energy limit of the string theory and dimensionally reduced Klein-Kaluza theory. It turns out that the value of the dilaton coupling does not influence the static configurations. However, the brane location in the black object spacetime is connected with the dimensionality of the spacetime in question. The brane bend in the nearby of the black object event horizon disappears closer to it as the dimensionality of the bulk increases. The possible explanation of this fact is connected with the gravity feature which can penetrate the additional dimensions. The same force (bounded

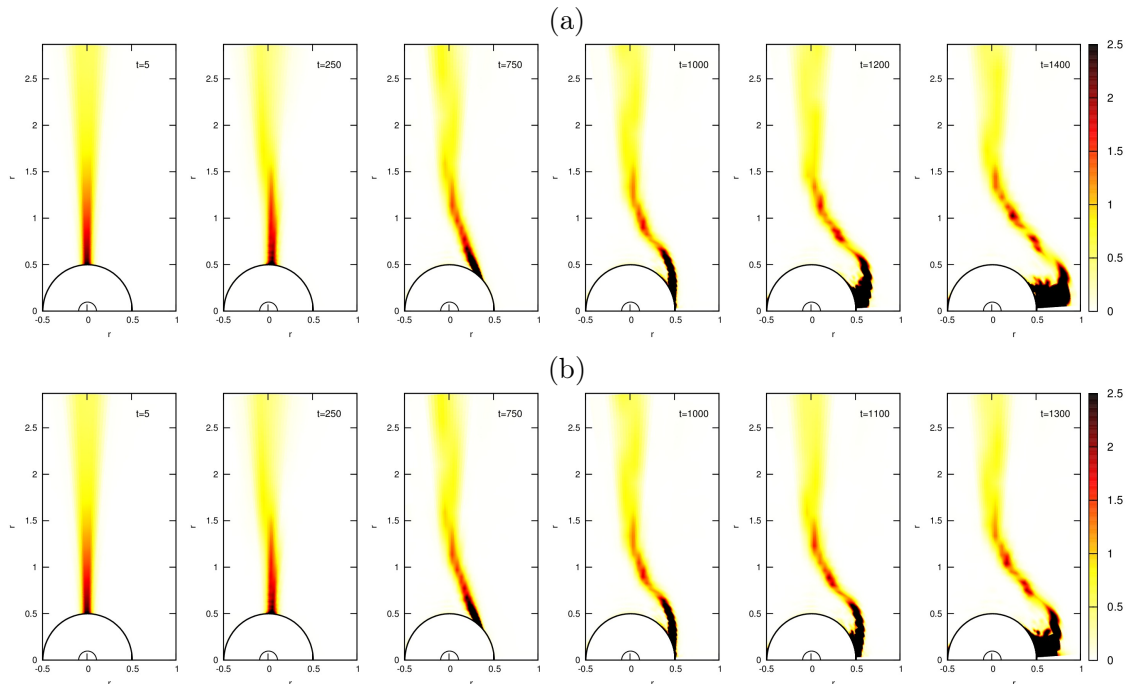


Figure 7. The evolution of the BDBH system with the nonextremal black hole for α equal to (a) -1 and (b) 0 . The remaining parameters were set as $d = 7$, $l = 0.1$ and $v = 0.3$.

with the black hole mass) ought to act in the additional dimensions and therefore is weaker in comparison to the four-dimensional case. Thus one can draw a conclusion that, the larger dimensionality of the spacetime manifold one considers, the weaker force is exerted on the brane in question.

In the case of the extremal dilaton black hole-brane configurations, one always gets expulsion of the brane from the black objects, disregarding dimension of the spacetime and the coupling constant of the theory under consideration. This fact confirms the previous results obtained for the four-dimensional dilaton black hole-brane system [18]. In four dimensions the same effect was also revealed for the Abelian Higgs cosmic strings and extremal dilaton black holes [46, 47].

The dynamical evolution of the examined system in the presence of both nonextremal and extremal black hole results in its expulsion from the brane. Similarly to the static configurations, the dilatonic coupling constant α also does not influence the process. The black hole is expelled earlier from the brane in bulk spacetimes of a bigger dimension and when the brane is thicker.

Acknowledgments

A.N., R.M. and M.R. were partially supported by the Polish National Science Centre grant no. DEC-2014/15/B/ST2/00089. Ł.N. was supported by the Polish National Science Centre under postdoctoral scholarship FUGA DEC-2014/12/S/ST2/00332.

References

- [1] N. Arkani-Hamed, S. Dimopoulos and G. R. Dvali, *The hierarchy problem and new dimensions at a millimeter*, *Phys. Lett. B* **429** (1998) 263.
- [2] N. Arkani-Hamed, S. Dimopoulos and G. R. Dvali, *Phenomenology, astrophysics, and cosmology of theories with submillimeter dimensions and TeV scale quantum gravity*, *Phys. Rev. D* **59** (1999) 086004.
- [3] L. Randall and R. Sundrum, *Large Mass Hierarchy from a Small Extra Dimension*, *Phys. Rev. Lett.* **83** (1999) 3370.
- [4] L. Randall and R. Sundrum, *An Alternative to Compactification*, *Phys. Rev. Lett.* **83** (1999) 4690.
- [5] N. Tanahashi and T. Tanaka, *Black Holes in Braneworlds Models*, *Prog. Theor. Phys. Suppl.* **189** (2011) 227.
- [6] V. P. Frolov, *Merger transitions in brane-black hole systems: Criticality, scaling, and self-similarity*, *Phys. Rev. D* **74** (2006) 044006.
- [7] B. Kol, *Topology change in general relativity, and the black-hole black-string transition*, *JHEP* **10** (2005) 049.
- [8] B. Kol, *The phase transition between caged black holes and black strings*, *Phys. Reports* **422** (2006) 119.
- [9] D. Mateos, R. C. Myers and R. M. Thomson, *Holographic Phase Transitions with Fundamental Matter*, *Phys. Rev. Lett.* **97** (2006) 091601.
- [10] D. Mateos, R. C. Myers and R. M. Thomson, *Thermodynamics of the brane*, *JHEP* **05** (2007) 067.
- [11] S. Dimopoulos and G. L. Landsberg, *Black holes at the LHC*, *Phys. Rev. Lett.* **87** (2001) 161602.
- [12] S. B. Giddings and S. Thomas, *High energy colliders as black hole factories: The end of short distance physics*, *Phys. Rev. D* **65** (2002) 056010.
- [13] A. Vilenkin and E. P. Shellard, *Cosmic strings and other topological defects*, (Cambridge University Press 1994).
- [14] S. Higaki, A. Ishibashi, and D. Ida, *Instability of a membrane intersecting a black hole*, *Phys. Rev. D* **63** (2000) 025002.
- [15] Y. Morisawa, R. Yamazaki, D. Ida, A. Ishibashi, and K. Nakao, *Thick domain walls intersecting a black hole*, *Phys. Rev. D* **62** (2000) 084022.
- [16] Y. Morisawa, R. Yamazaki, D. Ida, A. Ishibashi, and K. Nakao, *Thick domain walls around a black hole*, *Phys. Rev. D* **67** (2003) 025017.
- [17] M. Rogatko, *Dilaton black holes on thick branes*, *Phys. Rev. D* **64** (2001) 064014.
- [18] R. Moderski and M. Rogatko, *Thick domain walls and charged dilaton black holes*, *Phys. Rev. D* **67** (2003) 024006.
- [19] R. Moderski and M. Rogatko, *Reissner-Nordström black holes and thick domain walls*, *Phys. Rev. D* **69** (2004) 084018.
- [20] R. Moderski and M. Rogatko, *Thick domain walls in AdS black hole spacetimes*, *Phys. Rev. D* **74** (2006) 044002.

- [21] M. Rogatko, *Cosmological black holes on branes*, *Phys. Rev. D* **69** (2004) 044022.
- [22] A. Flachi and T. Tanaka, *Escape of black holes from the brane*, *Phys. Rev. Lett.* **95** (2005) 161302.
- [23] A. Flachi, O. Pujolas, M. Sasaki and T. Tanaka, *Black holes escaping from domain walls*, *Phys. Rev. D* **73** (2006) 125017.
- [24] A. Flachi, O. Pujolas, M. Sasaki and T. Tanaka, *Critical escape velocity of black holes from branes*, *Phys. Rev. D* **74** (2006) 045013.
- [25] A. Flachi and T. Tanaka, *Branes and black holes collision*, *Phys. Rev. D* **76** (2007) 025007.
- [26] A. Chamblin and D. M. Eardley, *Puncture of gravitating domain walls*, *Phys. Lett. B* **475** (2000) 46.
- [27] D. Stojkovic, K. Freese and G. D. Starkman, *Holes in the walls: Primordial black holes as a solution to the cosmological domain wall problem*, *Phys. Rev. D* **72** (2005) 045012.
- [28] V. G. Czimmer and A. Flachi, *Curvature corrections and topology change transition in brane-black hole systems: A perturbative approach*, *Phys. Rev. D* **80** (2009) 104017.
- [29] V. G. Czimmer, *Thick-brane solutions and topology change transition on black hole backgrounds*, *Phys. Rev. D* **82** (2010) 024035.
- [30] V. G. Czimmer, *A topologically flat thick 2-brane on higher-dimensional black hole backgrounds*, *Phys. Rev. D* **83** (2011) 064026.
- [31] V. Balek and B. Novotny, *Evolution of a black hole inhabited brane close to reconnection*, *Phys. Rev. D* **83** (2011) 024013.
- [32] D. V. Gal'tsov, E. Yu. Melkumova and P. Spirin, *Perforation of a domain wall by a point mass*, *Phys. Rev. D* **89** (2014) 085017.
- [33] D. V. Gal'tsov, E. Yu. Melkumova and P. Spirin, *Energy-momentum balance in a particle domain wall perforating collision*, *Phys. Rev. D* **90** (2014) 125024.
- [34] G. W. Gibbons, K.-i. Maeda, *Black holes and membranes in higher-dimensional theories with dilaton fields*, *Nucl. Phys. B* **298** (1988) 741.
- [35] P. A. M. Dirac, *An Extensible Model of the Electron*, *Proc. R. Soc. London, Ser. A* **268** (1962) 57.
- [36] J. Nambu, Copenhagen Summer Symposium (1970), unpublished.
- [37] T. Goto, *Merger Transitions in Brane-Black Hole Systems: Criticality, Scaling, and Self-Similarity*, *Prog. Theor. Phys.* **46** (1971) 1560.
- [38] G.W.Gibbons, M.Rogatko, and A.Szyplowska, *Decay of massive Dirac hair on a brane-world black hole*, *Phys. Rev. D* **77** (2008) 064024.
- [39] M.Rogatko, and A.Szyplowska, *Massive fermion emission from higher dimensional black holes*, *Phys. Rev. D* **79** (2009) 104005.
- [40] G.W.Gibbons and M.Rogatko, *Decay of Dirac hair around a dilaton black hole*, *Phys. Rev. D* **77** (2008) 044034.
- [41] J. P. Boyd, *Chebyshev and Fourier spectral methods*, Dover Publications 2000, NY, USA.
- [42] J. M. Maldacena, *The large- N limit of superconformal field theories and supergravity*, *Adv. Theor. Math. Phys.* **2** (1998) 231.

- [43] E. Witten, *Anti-de-Sitter space and holography*, *Adv. Theor. Math. Phys.* **2** (1998) 253.
- [44] S. S. Gubser, I. R. Klebanov and A. M. Polyakov, *Gauge theory correlators from noncritical string theory*, *Phys. Lett. B* **428** (1998) 105.
- [45] W. H. Press, S. A. Teukolsky, W. T. Vetterling, B. P. Flannery, *Numerical Recipes in Fortran 77*, Cambridge University Press 1997, USA.
- [46] R. Moderski and M. Rogatko, *Abelian Higgs hair for electrically charged dilaton black holes*, *Phys. Rev. D* **58** (1998) 124016.
- [47] R. Moderski and M. Rogatko, *The question of Abelian Higgs hair expulsion from extremal dilaton black holes*, *Phys. Rev. D* **60** (1999) 104040.